

# Two-loop gradient-flow renormalization of scalar QCD

Janosch Borgulat, Nils Felten, Robert V. Harlander, and Jonas T. Kohnen

*TTK, RWTH Aachen University, 52056 Aachen, Germany*

## Abstract

The gradient-flow formalism is applied to a non-Abelian gauge theory with scalar and fermionic particles, dubbed “scalar QCD”. It is shown that the flowed scalar quark requires a field renormalization, albeit only beyond the one-loop level. A pseudo-physical,  $t$ -dependent renormalization scheme is defined, and the corresponding renormalization constant is evaluated at the two-loop level. We also calculate the gluon action density as well as the condensate of the scalar and the fermionic quark at three-loop level in this theory. The results validate the consistency of the gradient-flow formalism in this theory and provide a further step towards applying the gradient-flow formalism to the full Standard Model.

## Contents

<b>1</b>	<b>Introduction</b>	<b>2</b>
<b>2</b>	<b>Flow equations and Feynman rules</b>	<b>3</b>
<b>3</b>	<b>Renormalization constants</b>	<b>6</b>
3.1	The strong coupling of scalar QCD in the gradient-flow scheme . . . . .	7
3.2	The flowed fermionic field renormalization . . . . .	10
3.3	The flowed scalar field renormalization . . . . .	11
<b>4</b>	<b>Short-flow-time expansions</b>	<b>13</b>
4.1	The scalar bilinear . . . . .	13
4.2	The Noether current . . . . .	15
<b>5</b>	<b>Flowed anomalous dimension</b>	<b>16</b>
<b>6</b>	<b>Conclusions and Outlook</b>	<b>17</b>
<b>A</b>	<b>Renormalization constants</b>	<b>18</b>
<b>B</b>	<b>Ancillary file</b>	<b>19</b>

# 1 Introduction

The gradient flow is an established tool in lattice gauge theory calculations [1–5]. It evolves the regular four-dimensional fields into an auxiliary dimension, the flow time  $t$ , according to a differential equation which is of first order in  $t$ . The effect of this evolution is a suppression of the fields' high-momentum modes, and thus a regularization of the associated ultra-violet (UV) divergences.

Aside from an efficient method to determine the lattice spacing [2,6], or a non-perturbative definition of the renormalized strong coupling [2], the gradient-flow formalism (GFF) also provides a way to facilitate the calculation and renormalization of operator matrix elements on the lattice, as well as their combination with perturbatively evaluated Wilson coefficients. A particularly welcome feature of the GFF is that it evades complications due to the breaking of Poincaré invariance on the lattice. This opens efficient ways to compute matrix elements of the energy momentum tensor on the lattice, for example [7,8], and most recently higher moments of parton densities [9,10]. A key to these methods is the so-called short-flow-time expansion (SFTX), which allows one to express composite operators of the flowed fields in terms of linear combinations of the regular operators. Proofs of the viability of this method have been provided in Refs. [10–15]. It requires perturbative matching coefficients between flowed and regular operators whose calculation leads to non-standard Feynman diagrams and integrals. Nevertheless, the standard methods for perturbative QCD calculations can be adapted to render such calculations possible at next-to-next-to-leading order (NNLO) and possibly even beyond that [16–23].

Understandably, the majority of such applications has been focused on QCD up to now. However, it is worth to consider also other theories, be it for theoretical reasons or due to their phenomenological relevance, for example in combination with effective field theories. Generalizations of the GFF have been considered in the context of super-Yang-Mills and other supersymmetric theories [24–31], or scalar theories in three and four space-time dimensions [32–36], for example.

In this paper, we consider the extension of QCD by the inclusion of scalar quarks. While the phenomenological relevance of the literal interpretation of this theory is doubtful in the light of current Large Hadron Collider (LHC) data, our results will be presented for a general non-Abelian compact gauge group with a scalar field and an arbitrary number of fermionic matter fields transforming in the corresponding irreducible representation. They can therefore be easily interpreted in terms of the unbroken weak sector of the Standard Model (SM), for example, and represent an important step towards a gradient-flow formulation of the full SM. Nevertheless, for the sake of convenience, we will refer to the underlying theory as scalar quantum chromodynamics (SQCD) in this paper, to the gauge bosons as gluons, and to the fermionic and scalar matter fields as quarks and squarks (or scalar quarks), respectively.

While the generalization of the flow equations to SQCD is straightforward, and the renormalization of the strong and the scalar coupling is the same as in regular SQCD and can be found in the literature, we will for the first time compute the flowed field renormalizations of the quarks and the squarks in this theory, up to two-loop level. In addition to the  $\overline{\text{MS}}$  scheme, they will be presented in the so-called ringed scheme which is suitable also for

a lattice realization. As a first application, we will also determine the SFTX of the two squark bilinear operators, namely the scalar and the Noether current.

The remainder of this paper is structured as follows. In the next section, we define the flow equations for SQCD and provide the relevant Feynman rules. Subsequently, the conceptual aspects for the renormalization of the strong coupling and the flowed fields is discussed, and the relevant renormalization constants are computed through NNLO in the strong and the scalar coupling. As an application, we study the SFTX of the scalar bilinear operator and the Noether current for the scalar quarks, computing the matching coefficients to the corresponding regular operators through NNLO in Section 4. The resulting flowed anomalous dimensions of these operators are discussed in Section 5, before we present an outlook and our conclusions in Section 6. In Appendix A, we collect the explicit results for the  $\beta$ -functions which are relevant for this paper, and in Appendix B, we describe the contents of the ancillary file which accompanies this paper, and which provides our main results in electronic form.

## 2 Flow equations and Feynman rules

We consider a gauge theory with a single scalar  $\phi$  (squark) and  $n_f$  fermions  $\psi_f$  (quarks), all transforming in the fundamental representation of the gauge group. Including the gauge-fixing terms and the corresponding Faddeev-Popov ghosts  $c, \bar{c}$ , the Lagrangian reads

$$\begin{aligned}\mathcal{L}_{\text{SQCD}} &= \mathcal{L}_{\text{QCD}} + \mathcal{L}_\phi, \\ \mathcal{L}_{\text{QCD}} &= -\frac{1}{4}F_{\mu\nu}^a F_{\mu\nu}^a + \sum_{f=1}^{n_f} \bar{\psi}_f \not{D}^F \psi_f + \frac{1}{2\xi}(\partial_\mu A_\mu^a)^2 + \partial_\mu \bar{c}^a D_\mu^{ab} c^b, \\ \mathcal{L}_\phi &= (D_\mu^F \phi)^\dagger (D_\mu^F \phi) - \frac{\lambda_B}{4}(\phi^\dagger \phi)^2.\end{aligned}\tag{2.1}$$

Here,  $A_\mu^a$  are the gauge fields (gluons),

$$D_\mu^F = \partial_\mu + g_B A_\mu^a t^a, \quad D_\mu^{ab} = \delta^{ab} \partial_\mu - g_B f^{abc} A_\mu^c,\tag{2.2}$$

are the covariant derivatives in the fundamental and the adjoint representation, respectively, and

$$F_{\mu\nu}^a = \partial_\mu A_\nu^a - \partial_\nu A_\mu^a + g_B f^{abc} A_\mu^b A_\nu^c\tag{2.3}$$

is the field strength tensor. The  $t^a$  are the generators of the gauge group in the fundamental representation, and the  $f^{abc}$  are the structure constants. We follow the conventions of Refs. [4, 18], which means that

$$[t^a, t^b] = f^{abc} t^c, \quad \text{Tr}(t^a t^b) = -T_R \delta^{ab},\tag{2.4}$$

with the trace normalization  $T_R$  to be specified below. It is convenient to define the combinations

$$a_s^B = \frac{g_B^2}{4\pi^2}, \quad a_\lambda^B = \frac{\lambda_B}{4\pi^2},\tag{2.5}$$

where  $g_B$  and  $\lambda_B$  denote the bare coupling constants of the theory. Unless required, we will suppress the flavor indices  $f$  on the quark fields in the following.

The gradient flow evolves the fields into an auxiliary dimension, the so-called flow time  $t$ . The evolution is governed by the flow equation, which is a first-order differential equation in  $t$ , and associated ‘‘initial conditions’’, which establish the contact to the regular fields at  $t = 0$ . In the case of the flowed gluon and quark fields  $B_\mu$ ,  $\chi$ , and  $\bar{\chi}$ , the flow equations are given by

$$\begin{aligned} 0 &= \partial_t B_\mu^a - \mathcal{D}_\nu^{ab} G_{\mu\nu}^b - \kappa \mathcal{D}_\mu^{ab} \partial_\nu B_\nu^b && \equiv \mathcal{F}_B^a, \\ 0 &= \partial_t \chi - \Delta \chi + g_B \kappa \partial_\mu B_\mu^a t^a \chi && \equiv \mathcal{F}_\chi, \\ 0 &= \partial_t \bar{\chi} - \bar{\chi} \overleftarrow{\Delta} - g_B \kappa \bar{\chi} \partial_\mu B_\mu^a t^a && \equiv \bar{\mathcal{F}}_\chi, \end{aligned} \quad (2.6)$$

and the initial conditions are

$$\begin{aligned} B_\mu^a(t=0, x) &= A_\mu^a(x), \\ \chi(t=0, x) &= \psi(x), \\ \bar{\chi}(t=0, x) &= \bar{\psi}(x). \end{aligned} \quad (2.7)$$

The gauge parameter  $\kappa$  will be chosen equal to one in our calculations. The flowed field-strength tensor is given by

$$G_{\mu\nu}^a = \partial_\mu B_\nu^a - \partial_\nu B_\mu^a + g_B f^{abc} B_\mu^b B_\nu^c, \quad (2.8)$$

and the covariant derivatives in the fundamental and adjoint representation are defined as

$$\mathcal{D}_\mu^F = \partial_\mu + g_B B_\mu^a t^a, \quad \overleftarrow{\mathcal{D}}_\mu^F = \overleftarrow{\partial}_\mu - g_B B_\mu^a t^a, \quad \mathcal{D}_\mu^{ab} = \delta^{ab} \partial_\mu - g_B f^{abc} B_\mu^c. \quad (2.9)$$

Furthermore, we introduced the short-hand notation

$$\Delta = \mathcal{D}_\mu^F \mathcal{D}_\mu^F, \quad \overleftarrow{\Delta} = \overleftarrow{\mathcal{D}}_\mu^F \overleftarrow{\mathcal{D}}_\mu^F. \quad (2.10)$$

For the flowed scalar fields  $\varphi$ ,  $\varphi^\dagger$ , we employ the following flow equations (see also Refs. [32, 35]):

$$\begin{aligned} 0 &= \partial_t \varphi - \Delta \varphi + g_B \kappa \partial_\mu B_\mu^a t^a \varphi && \equiv \mathcal{F}_\varphi, \\ 0 &= \partial_t \varphi^\dagger - \varphi^\dagger \overleftarrow{\Delta} - g_B \kappa \varphi^\dagger \partial_\mu B_\mu^a t^a && \equiv \mathcal{F}_\varphi^\dagger, \end{aligned} \quad (2.11)$$

with the boundary conditions

$$\begin{aligned} \varphi(t=0, x) &= \phi(x), \\ \varphi^\dagger(t=0, x) &= \phi^\dagger(x). \end{aligned} \quad (2.12)$$

The flow equations can be implemented in the Lagrangian by introducing Lagrange multiplier fields  $L_\mu^a$ ,  $\lambda_f$ ,  $\bar{\lambda}_f$ ,  $\eta$ , and  $\eta^\dagger$ , and defining

$$\begin{aligned} \mathcal{L}_B &= -2 \int_0^\infty dt \operatorname{Tr} \left[ L_\mu^a \mathcal{F}_B^a \right], \\ \mathcal{L}_\chi &= \int_0^\infty dt \left[ \bar{\lambda} \mathcal{F}_\chi + \bar{\mathcal{F}}_\chi \lambda \right], \\ \mathcal{L}_\varphi &= \int_0^\infty dt \left[ \eta^\dagger \mathcal{F}_\varphi + \mathcal{F}_\varphi^\dagger \eta \right], \end{aligned} \quad (2.13)$$

where summation over flavor indices is understood. The flowed Lagrangian then reads

$$\mathcal{L} = \mathcal{L}_{\text{SQCD}} + \mathcal{L}_B + \mathcal{L}_\chi + \mathcal{L}_\varphi, \quad (2.14)$$

where the first term notes the regular (i.e., unflowed) part of the Lagrangian given in Eq. (2.1), and the remaining terms incorporate the flow equations in Eqs. (2.6) and (2.11).

Using Eqs. (2.13) and (2.14), one can derive Feynman rules for the flowed fields along the lines of Ref. [4]. In addition to generalized propagators for the flowed fields, they also involve so-called *flow lines*, corresponding to mixed two-point functions of the flowed field and its associated Lagrange multiplier. They couple to one another or to flowed fields via *flowed vertices* which involve integrations over flow-time parameters. For details, we refer to Ref. [18], where also the complete set of Feynman rules for the non-scalar part of Eq. (2.14) can be found. For the regular SQCD Feynman rules involving scalars, on the other hand, we use<sup>1</sup>

$$\begin{aligned}
 & \begin{array}{c} \bullet \\ s, j \end{array} \begin{array}{c} \xrightarrow{p} \\ \text{---} \\ \xrightarrow{p} \end{array} \begin{array}{c} \bullet \\ t, i \end{array} = \delta_{ij} \frac{1}{p^2} e^{-(t+s)p^2}, \\
 & \begin{array}{c} k \text{---} \\ \diagdown \\ \bullet \\ \diagup \\ l \text{---} \end{array} \begin{array}{c} \text{---} \\ \diagup \\ \bullet \\ \diagdown \\ \text{---} \end{array} \begin{array}{c} i \\ \text{---} \\ \diagdown \\ \bullet \\ \diagup \\ j \text{---} \end{array} = -\frac{\lambda^B}{2} (\delta_{ij} \delta_{kl} + \delta_{il} \delta_{jk}), \\
 & \begin{array}{c} \text{---} \\ \text{---} \\ \text{---} \\ \text{---} \\ \text{---} \\ \text{---} \\ \text{---} \\ \text{---} \\ \text{---} \\ \text{---} \\ \text{---} \\ \bullet \\ \mu, a \end{array} \begin{array}{c} \xrightarrow{p} \\ \text{---} \\ \xrightarrow{q} \end{array} \begin{array}{c} i \\ \text{---} \\ \diagdown \\ \bullet \\ \diagup \\ j \text{---} \end{array} = i g_B (t^a)_{ij} (p^\mu - q^\mu), \\
 & \begin{array}{c} \text{---} \\ \text{---} \\ \text{---} \\ \text{---} \\ \text{---} \\ \text{---} \\ \text{---} \\ \text{---} \\ \text{---} \\ \text{---} \\ \text{---} \\ \bullet \\ \mu, a \end{array} \begin{array}{c} \text{---} \\ \diagup \\ \bullet \\ \diagdown \\ \text{---} \end{array} \begin{array}{c} j \\ \text{---} \\ \diagdown \\ \bullet \\ \diagup \\ i \text{---} \end{array} = g_B^2 \{t^a, t^b\}_{ij} \delta_{\mu\nu}.
 \end{aligned} \quad (2.15)$$

Here,  $i, j, k, l$  are color indices of the fundamental representation,  $a, b$  are color indices of the adjoint representation,  $\mu, \nu$  are Lorentz indices,  $s$  and  $t$  are flow-time variables, and the momenta  $p$  and  $q$  are assumed outgoing. The Feynman rules for the flowed vertices

<sup>1</sup>All diagrams in this paper are produced with the help of FEYNGAME [37–39].

read

$$\begin{aligned}
 & \text{Diagram 1: } i = ig_B(t^a)_{ij} \int_0^\infty ds (2p_\mu + (1 - \kappa)q_\mu) , \\
 & \text{Diagram 2: } i = -ig_B(t^a)_{ji} \int_0^\infty ds (2p_\mu + (1 - \kappa)q_\mu) , \\
 & \text{Diagram 3: } i = g_B^2 \{t^a, t^b\}_{ij} \delta_{\mu\nu} \int_0^\infty ds , \\
 & \text{Diagram 4: } i = g_B^2 \{t^a, t^b\}_{ij} \delta_{\mu\nu} \int_0^\infty ds ,
 \end{aligned}
 \tag{2.16}$$

where the arrows next to the lines, indicating that the corresponding line is a flow line, point towards increasing flow time. Dashed arrows indicate that the line can be a flowed propagator or a flow line.

### 3 Renormalization constants

It is well known that the renormalization of the fundamental parameters of the flowed Lagrangian is the same as for the regular theory [4]. Since we assume the quarks and the squark to be massless, the only fundamental parameters of our theory are the coupling constants  $a_s^B$  and  $a_\lambda^B$ . Their renormalization in SQCD is known through three-loop level [40] in the  $\overline{\text{MS}}$  scheme, which, however, is only defined perturbatively. The GFF, on the other hand, allows for a definition of the strong coupling which can be implemented both perturbatively and non-perturbatively:

$$\frac{\alpha_s^{\text{GF}}(t)}{\pi} \equiv a_s^{\text{GF}}(t) = \frac{E(t)}{E_0(t)}, \quad \text{with} \quad E_0(t) = \frac{3n_A}{32t^2}, \tag{3.1}$$

where

$$E(t) = \frac{g_B^2}{4} \langle G_{\mu\nu}^a(t) G_{\mu\nu}^a(t) \rangle \tag{3.2}$$

is the gluon action density, and  $n_A$  is the dimension of the adjoint representation of the gauge group. The perturbative expression for  $E(t)$  within QCD, and thus the conversion between the  $\overline{\text{MS}}$  and the GF scheme, is currently known through NNLO [16] and has been used for a novel extraction of the QCD scale  $\Lambda_{\text{QCD}}$  in the  $\overline{\text{MS}}$  scheme [41] and the  $\overline{\text{MS}}$  coupling  $\alpha_s(M_Z)$  [42]. In Section 3.1, we will generalize this result to SQCD. A similar non-perturbative definition is also possible for the scalar coupling  $\alpha_\lambda$ , of course, but it requires the calculation of  $\langle(\phi^\dagger\phi)^2\rangle$ , which is beyond the scope of the current paper.

Concerning the renormalization of the flowed fields, we write

$$\begin{aligned} B_\mu^{a,\text{R}} &= Z_B^{1/2} B_\mu^a, \\ \chi_f^{\text{R}} &= Z_\chi^{1/2} \chi_f, \quad \bar{\chi}_f^{\text{R}} = Z_\chi^{1/2} \bar{\chi}_f, \\ \varphi^{\text{R}} &= Z_\varphi^{1/2} \varphi, \quad \varphi^{\dagger,\text{R}} = Z_\varphi^{1/2} \varphi^\dagger. \end{aligned} \tag{3.3}$$

It was shown in QCD that the flowed gluon does not require renormalization [4, 5], and since the same arguments apply to SQCD, we can set  $Z_B = 1$  to all orders in perturbation theory.

On the other hand, the flowed quark field turns out to require a non-trivial renormalization  $Z_\chi$ . A particularly useful renormalization condition which can be implemented both on the lattice and in perturbation theory is the so-called ringed scheme, defined as

$$\mathring{Z}_\chi \sum_{f=1}^{n_f} \langle \bar{\chi}_f(t) \mathcal{D}^{\text{F}} \chi_f(t) \rangle = -\frac{2n_c n_f}{(4\pi t)^2}, \tag{3.4}$$

where  $n_c$  is the dimension of the fundamental representation of the gauge group. In QCD,  $\mathring{Z}_\chi$  is known through NNLO [5, 18]. In this paper, we will generalize this result to SQCD, see Section 3.2.

The flowed squark renormalization  $Z_\varphi$  has not been considered before. Its NNLO expression will be one of the main results of our calculation. We provide it in a scheme analogous to the fermionic case by requiring the renormalization condition

$$\mathring{Z}_\varphi \langle \varphi^\dagger(t) \varphi(t) \rangle \equiv \frac{n_c}{32\pi^2 t}, \tag{3.5}$$

where the r.h.s. is defined such that  $\mathring{Z}_\varphi = 1 + \text{higher orders}$ .

### 3.1 The strong coupling of scalar QCD in the gradient-flow scheme

In order to generalize the result for Eq. (3.2) to SQCD, we need to take into account diagrams with closed squark loops. The only such diagram which gives a non-zero contribution up to the two-loop level is shown in Fig. 1 (a); all others which could be generated from the Feynman rules vanish because they lead to scaleless loop integrals. Two three-loop diagrams with squark loops are shown in Fig. 1 (b),(c). Since the associated loop integrals are UV divergent before the renormalization of  $\alpha_s$ , we adopt dimensional regularization and evaluate them in  $D = 4 - 2\epsilon$  space-time dimensions.

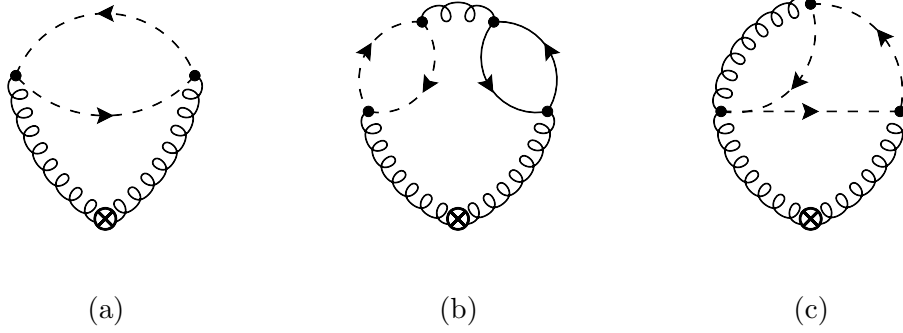


Figure 1: Contributions to  $E(t)$  involving squarks at (a) NLO and (b), (c) NNLO. The spiral lines are gluons, the dashed lines are squarks, and the solid lines are quarks. The lower vertex marked  $\otimes$  denotes the flowed operator  $G_{\mu\nu}(t)G^{\mu\nu}(t)$ , the other vertices are regular QCD vertices.

All calculations in this paper are carried out by using the tool chain first described in Ref. [18], albeit slightly updated. It is based on `qgraf` [43, 44] for the generation of the Feynman diagrams, `tapir` [45] for inserting the Feynman rules, `exp` [46] for the identification of the integral topologies, `FORM` [47, 48] for all algebraic operations, and `Kira+FireFly` [49–53] for the reduction to master integrals. At two-loop level, all master integrals are known in analytic form [2, 17]. At three-loop level, we evaluate the master integrals using `ftint` [23], which uses `pySecDec` [54–57] to perform a sector decomposition [58, 59] and to evaluate the coefficients of the Laurent series in  $\epsilon$  numerically.

After renormalization of the strong coupling according to Eq. (A.1), we obtain the result

$$E(t) = a_s E_0(t) (1 + e_1 + e_2 + \text{h.o.}) \quad (3.6)$$

with

$$e_n = \sum_{i=0}^n \left[ e_{i,n-i} + e_{i,n-i}^{(1l)} L_{\mu t} + \cdots + e_{i,n-i}^{(nl)} L_{\mu t}^n \right] a_s^i a_\lambda^{n-i}, \quad (3.7)$$

and

$$L_{\mu t} = \ln 2\mu^2 t + \gamma_E \equiv \ln \frac{\mu^2}{\mu_t^2}, \quad (3.8)$$

where  $\gamma_E = -\Gamma'(1) = 0.577216\dots$  is the Euler-Mascheroni constant, and we have implicitly defined the  $t$ -dependent energy scale  $\mu_t$ . Here and in the following,  $a_s$  and  $a_\lambda$  denote the  $\overline{\text{MS}}$  renormalized couplings defined in Eq. (A.1), with their dependence on the renormalization scale  $\mu$  suppressed, and “h.o.” (for “higher orders”) denotes terms of order  $a_s^i a_\lambda^j$ , with  $i + j \geq 3$ . For the constant terms up to three-loop level ( $n \leq 2$ ) in Eq. (3.7), we obtain

$$\begin{aligned} e_{10} &= e_{10}^{\text{QCD}} - \frac{5}{36} T_R, \\ e_{20} &= e_{20}^{\text{QCD}} - T_R [0.7639 C_A + 0.34532 C_F - T_R (0.0976 n_f + 0.0238)], \\ e_{ij} &= 0 \quad \text{otherwise,} \end{aligned} \quad (3.9)$$



where the color factors are

$$C_F = T_R \frac{n_c^2 - 1}{n_c}, \quad C_A = 2T_R n_c, \quad T_R = \frac{1}{2}. \quad (3.10)$$

The coefficients  $e_{10}^{\text{QCD}}$  and  $e_{20}^{\text{QCD}}$  correspond to the pure QCD result as obtained in Ref. [16, 18]. Since we adopt a different normalization in this paper, let us quote them again here:

$$\begin{aligned} e_{10}^{\text{QCD}} &= \left( \frac{13}{9} + \frac{11}{6} \ln 2 - \frac{3}{4} \ln 3 \right) C_A - \frac{2}{9} T_R n_f \\ e_{20}^{\text{QCD}} &= 1.74865 C_A^2 - (1.97283 \dots) T_R C_A n_f \\ &\quad + \left( \zeta_3 - \frac{43}{48} \right) T_R C_F n_f + \left( \frac{1}{9} \zeta_2 - \frac{5}{81} \right) T_R^2 n_f^2, \end{aligned} \quad (3.11)$$

where  $\zeta_n \equiv \sum_{k=1}^{\infty} 1/k^n$  is Riemann's zeta function with  $\zeta_2 = \pi^2/6 = 1.64493\dots$  and  $\zeta_3 = 1.20206\dots$ . The exact expression for the  $T_R C_A n_f$  term can be found in Ref. [18].

The logarithmic terms of Eq. (3.7) can be derived from the renormalization-group equation (RGE)

$$\mu^2 \frac{d}{d\mu^2} E(t) = \left[ \frac{\partial}{\partial L_{\mu t}} + \beta^s(a_s, a_\lambda) \frac{\partial}{\partial a_s} + \beta^\lambda(a_s, a_\lambda) \frac{\partial}{\partial a_\lambda} \right] E(t) = 0, \quad (3.12)$$

with the beta functions  $\beta^s$  and  $\beta^\lambda$  defined in Eq. (A.2). For  $n \leq 2$ , this leads to

$$\begin{aligned} e_{10}^{(1l)} &= \beta_{20}^s, & e_{20}^{(1l)} &= \beta_{30}^s + 2\beta_{20}^s e_{10}, & e_{20}^{(2l)} &= (\beta_{20}^s)^2, \\ e_{ij}^{(nl)} &= 0 & & \text{otherwise.} & & \end{aligned} \quad (3.13)$$

The coefficients  $\beta_{ij}^s$  are collected in Eq. (A.3).

Since  $E(t)$  and the strong beta function in the  $\overline{\text{MS}}$  scheme are independent of  $a_\lambda$  through three-loop level, our results allow us to evaluate the beta function of the strong coupling in SQCD in the gradient-flow scheme. In analogy to Eq. (A.2), we write

$$\mu^2 \frac{d}{d\mu^2} a_s^{\text{GF}}(\mu) = \beta^{\text{GF}}(a_s^{\text{GF}}, a_\lambda) \equiv -\epsilon a_s^{\text{GF}} - \sum_{n=0}^3 \beta_{n0}^{\text{GF}} (a_s^{\text{GF}})^n + \text{h.o.} \quad (3.14)$$

The first two perturbative coefficients are scheme independent, of course, thus

$$\beta_{20}^{\text{GF}} = \beta_{20}^s, \quad \beta_{30}^{\text{GF}} = \beta_{30}^s, \quad (3.15)$$

while the three-loop coefficient is given by

$$\beta_{40}^{\text{GF}} = \beta_{40}^s - e_{10} \beta_{30}^s + (e_{20} - e_{10}^2) \beta_{20}^s. \quad (3.16)$$

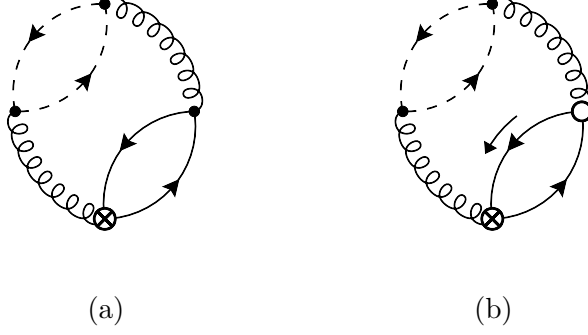


Figure 2: Contributions to  $\langle \bar{\chi}^\dagger(t) \not{D} \chi(t) \rangle$  involving squarks. The notation is the same as in Fig. 1, only that the vertex marked  $\otimes$  now denotes the operator  $\bar{\chi}^\dagger(t) \chi(t)$ . In addition, lines with an arrow next to them are the associated flow lines (the arrow denotes the flow direction), and the symbol  $\circ$  marks a flow vertex.

### 3.2 The flowed fermionic field renormalization

Additional diagrams beyond pure QCD which contribute to the vacuum expectation value (VEV) of Eq. (3.4) in SQCD occur only at three-loop level and beyond. Two examples are shown in Fig. 2. They affect the  $\overline{\text{MS}}$  part of the renormalization constant as well as the finite part which characterizes the ringed scheme. Writing

$$\mathring{Z}_\chi = \zeta_\chi Z_\chi, \quad (3.17)$$

where  $Z_\chi$  is the  $\overline{\text{MS}}$  renormalization, and adopting the notation of Eq. (A.8) for  $Z_\chi$ , we find for the  $\overline{\text{MS}}$  coefficients up to NNLO in  $a_s$  and  $a_\lambda$ :

$$\begin{aligned} \gamma_{\chi,10} &= \gamma_{\chi,10}^{\text{QCD}}, & \gamma_{\chi,20} &= \gamma_{\chi,20}^{\text{QCD}} + 0.1771 C_F T_R, \\ \gamma_{\chi,ij} &= 0 & \text{otherwise,} \end{aligned} \quad (3.18)$$

where  $\gamma_{\chi,ij}^{\text{QCD}}$  refers to the QCD results obtained in Refs. [5, 18]:

$$\begin{aligned} \gamma_{\chi,10}^{\text{QCD}} &= -\frac{3}{4} C_F, \\ \gamma_{\chi,20}^{\text{QCD}} &= \left( \frac{1}{2} \ln 2 - \frac{223}{96} \right) C_A C_F + \left( \frac{3}{32} + \frac{1}{2} \ln 2 \right) C_F^2 + \frac{11}{24} C_F T_R n_f. \end{aligned} \quad (3.19)$$

The conversion factor to the ringed scheme reads, in our notation,

$$\begin{aligned} \zeta_\chi &= 1 - a_s \left( \gamma_{\chi,10} L_{\mu t} + \frac{3}{4} C_F \ln 3 + C_F \ln 2 \right) \\ &+ a_s^2 \left\{ \frac{\gamma_{\chi,10}}{2} (\gamma_{\chi,10} - \beta_{20}^s) L_{\mu t}^2 + \left[ \gamma_{\chi,10} (\beta_{20}^s - \gamma_{\chi,10}) \ln 3 \right. \right. \\ &\left. \left. + \frac{4}{3} \gamma_{\chi,10} (\beta_{20}^s - \gamma_{\chi,10}) \ln 2 - \gamma_{\chi,20} \right] L_{\mu t} + \frac{c_\chi^{(2)}}{16} \right\} + \text{h.o.}, \end{aligned} \quad (3.20)$$

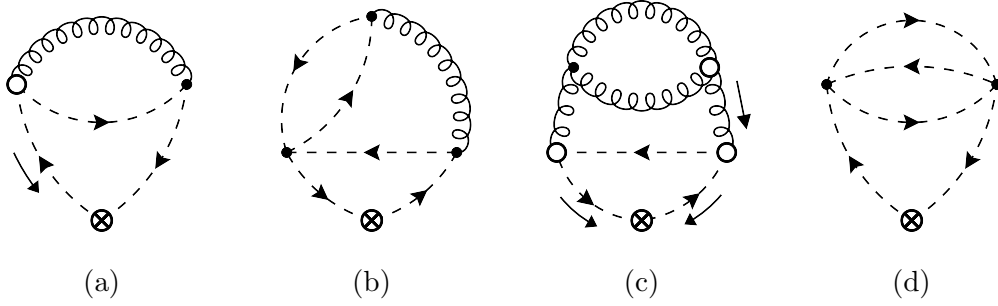


Figure 3: Contributions to  $\langle \varphi^\dagger(t)\varphi(t) \rangle$  at order  $a_s$ ,  $a_s a_\lambda$ ,  $a_s^2$ , and  $a_\lambda^2$  (a–d). The notation is the same as in Fig. 1. Lines with an arrow next to them denote flow lines. All “mixed” diagrams with both a quartic scalar and a gauge vertex such as diagram (b) evaluate to zero individually. Diagram (d) is the only non-vanishing three-loop diagram without a gauge coupling.

where  $\gamma_{\chi,ij}$  and  $\beta_{ij}^s$  are given in Eqs. (3.19) and (A.3).

For the non-logarithmic term at NNLO, we find

$$c_\chi^{(2)} = c_{\chi,\text{QCD}}^{(2)} - 0.3748 C_F T_R, \quad (3.21)$$

where the QCD part was obtained in Ref. [18]:

$$c_{\chi,\text{QCD}}^{(2)} = C_A C_F c_{\chi,A} + C_F^2 c_{\chi,F} + C_F T_R n_f c_{\chi,R}, \quad (3.22)$$

with<sup>2</sup>

$$\begin{aligned} c_{\chi,A} &= -23.7947, & c_{\chi,F} &= 30.3914, \\ c_{\chi,R} &= -\frac{131}{18} + \frac{46}{3}\zeta_2 + \frac{944}{9}\ln 2 + \frac{160}{3}\ln^2 2 - \frac{172}{3}\ln 3 + \frac{104}{3}\ln 2 \ln 3 \\ &\quad - \frac{178}{3}\ln^2 3 + \frac{8}{3}\text{Li}_2(1/9) - \frac{400}{3}\text{Li}_2(1/3) + \frac{112}{3}\text{Li}_2(3/4) = -3.92255\dots, \end{aligned} \quad (3.23)$$

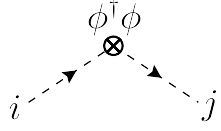
where  $\text{Li}_2(x)$  is the dilogarithm.

### 3.3 The flowed scalar field renormalization

Adopting the renormalization scheme defined in Eq. (3.5) for the scalar quark, we need to compute the scalar squark density up to three-loop level when aiming for the NNLO result. The relevant Feynman rules for the operator  $\varphi^\dagger(t)\varphi(t)$  is the same as for the regular

<sup>2</sup>The factor  $-1/18$  should read  $1/18$  in Eq. (B.3) of Ref. [18] (Eq. (131) in the arXiv version).

operator  $\phi^\dagger\phi$ :



$$= \delta_{ij}. \quad (3.24)$$

Sample diagrams contributing at NLO and NNLO are shown in Fig. 3. In analogy to the fermionic case, we factorize the ringed renormalization constant into an  $\overline{\text{MS}}$  part  $Z_\varphi$ , and a conversion factor  $\zeta_\varphi$ :

$$\mathring{Z}_\varphi = \zeta_\varphi Z_\varphi. \quad (3.25)$$

Adopting again Eq. (A.8), we find for the  $\overline{\text{MS}}$  coefficients through NNLO:

$$\begin{aligned} \gamma_{\varphi,20} &= C_F^2 \left( -\frac{3}{32} + \frac{11}{4} \ln 2 - \frac{9}{8} \ln 3 \right) + C_F C_A \left( -\frac{65}{64} - \frac{7}{4} \ln 2 + \frac{9}{8} \ln 3 \right) \\ &\quad + C_F T_R \left( \frac{1}{32} + \frac{1}{8} n_f \right), \\ \gamma_{\varphi,02} &= -\frac{1}{128} (n_c + 1), \quad \gamma_{\varphi,ij} = 0 \quad \text{otherwise.} \end{aligned} \quad (3.26)$$

This means that the squark field renormalization is only required at the two-loop level and beyond. The color factor  $(n_c + 1)$  of Eq. (3.26) arises from the contraction of the four-squark vertex with another pair of Kronecker- $\delta$ s; an overall factor  $n_c$  is taken into account in Eq. (3.5). Out of 377 three-loop diagrams, only the one shown in Fig. 3 (b) contributes to  $\gamma_{\varphi,02}$ . Remarkably, diagrams with both a scalar and a gauge coupling vanish individually at three-loop level, so that  $\gamma_{\varphi,11} = 0$  as indicated in Eq. (3.26).

For the conversion factor to the ringed scheme, we find

$$\begin{aligned} \zeta_\varphi &= 1 - a_s C_F (1 + 2 \ln 2) + a_s^2 \left\{ c_{\varphi,20}^{(2)} - L_{\mu t} [\gamma_{\varphi,20} + \beta_{20}^s C_F (1 + 2 \ln 2)] \right\} \\ &\quad + a_\lambda^2 [c_{\varphi,02}^{(2)} - L_{\mu t} \gamma_{\varphi,02}] + \text{h.o.}, \end{aligned} \quad (3.27)$$

where  $\beta_{20}^s$  is given in Eq. (A.3), and

$$\begin{aligned} c_{\varphi,20}^{(2)} &= 3.2133 C_F^2 - 4.268 C_A C_F + C_F T_R (1.086 n_f + 0.4547), \\ c_{\varphi,02}^{(2)} &= 0.025391 (n_c + 1). \end{aligned} \quad (3.28)$$

The logarithmic term is consistent with the RGE

$$\mu^2 \frac{d}{d\mu^2} \mathring{Z}_\varphi \langle \varphi^\dagger(t) \varphi(t) \rangle = 0, \quad (3.29)$$

from which one derives

$$\left[ \frac{\partial}{\partial L_{\mu t}} + \beta^s(\alpha_s, a_\lambda) \frac{\partial}{\partial \alpha_s} + \beta^\lambda(\alpha_s, a_\lambda) \frac{\partial}{\partial a_\lambda} - \gamma_\varphi(\alpha_s, a_\lambda) \right] \zeta_\varphi = 0, \quad (3.30)$$

where  $\gamma_\varphi$  is defined according to the generic form of Eq. (A.7), with the coefficients given in Eq. (3.26).

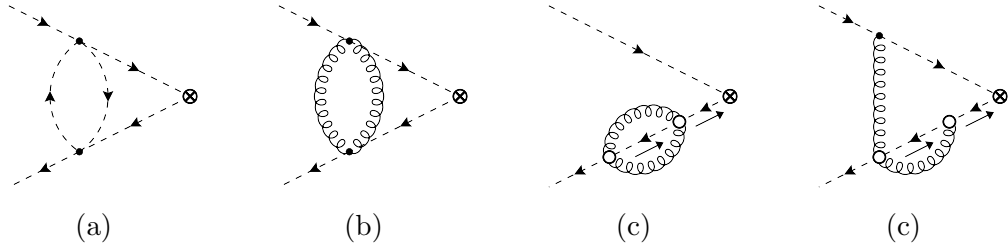


Figure 4: Sample diagrams contributing to the SFTX expansion of  $\varphi^\dagger(t)\varphi(t)$  at two-loop level. In total, we find 532 diagrams at this order (11 at one-loop level), including those which vanish due to closed flow-time loops.

## 4 Short-flow-time expansions

As an application of our results, we will derive the SFTX of two bilinear flowed squark operators.

### 4.1 The scalar bilinear

The first operator we consider is the scalar squark bilinear. Neglecting linear and higher terms in  $t$ , its SFTX takes the form

$$\mathring{Z}_\varphi \varphi^\dagger(t)\varphi(t) = \frac{1}{t}c_0(t)\mathbf{1} + c_1(t)Z_{\phi^\dagger\phi}\phi^\dagger\phi. \quad (4.1)$$

The coefficients  $c_0(t)$  and  $c_1(t)$  can be evaluated by applying the method of projectors [60] (see also Ref. [22], for example). It implies that  $c_0(t)$  is obtained from the VEV of the operator on the l.h.s. Using Eq. (3.5), it immediately follows that

$$c_0(t) = \frac{n_c}{32\pi^2} \quad (4.2)$$

to all orders in perturbation theory. The coefficient  $c_1(t)$  is determined by the matrix element of  $\varphi^\dagger\varphi$  with two external (regular)  $\phi$  fields, evaluated at zero momentum. Sample diagrams are shown in Fig. 4. Requiring  $c_1(t)$  to be finite determines the  $\overline{\text{MS}}$  renormalization constant  $Z_{\phi^\dagger\phi}$  for the unflowed operator  $\phi^\dagger\phi$  through two-loop level. As usual, we express it in terms of the perturbative coefficients of the anomalous dimension  $\gamma_{\phi^\dagger\phi}$ , see Eqs. (A.7) and (A.8), and find<sup>3</sup>

$$\begin{aligned} \gamma_{\phi^\dagger\phi,00} &= 0, & \gamma_{\phi^\dagger\phi,10} &= \frac{3}{4}C_F, & \gamma_{\phi^\dagger\phi,01} &= -\frac{1}{8}(n_c + 1), \\ \gamma_{\phi^\dagger\phi,20} &= -\frac{5}{32}C_F^2 + \frac{143}{192}C_A C_F - C_F T_R \left( \frac{71}{96} + \frac{5}{24}n_f \right), \\ \gamma_{\phi^\dagger\phi,02} &= \frac{5}{128}(n_c + 1), & \gamma_{\phi^\dagger\phi,11} &= -\frac{1}{4}C_F(n_c + 1). \end{aligned} \quad (4.3)$$

<sup>3</sup>There actually is a result for  $\gamma_{\phi^\dagger\phi}$  in the literature from more than 35 years ago [61], which, however, disagrees with our findings.

Since  $\gamma_{\phi^\dagger\phi}$  is related to the Higgs mass anomalous dimension in the Standard Model [62,63], we checked our result by reproducing the SU(2) part of the latter.

The renormalized expression for  $c_1(t)$  is then given by

$$c_1(t) = \sum_{n,m=0}^{\infty} c_{1,nm} a_s^n a_\lambda^m, \quad (4.4)$$

with coefficients up to NNLO ( $n + m = 2$ ) as

$$\begin{aligned} c_{1,00} &= 1, & c_{1,10} &= -C_F \left( \frac{5}{4} + 2 \ln 2 \right), & c_{1,01} &= \frac{1}{8} (n_c + 1), \\ c_{1,20} &= C_F^2 \left( -\frac{1}{32} - \frac{5}{32} \zeta_2 + \frac{47}{8} \ln 2 - \frac{7}{8} \ln^2 2 + \frac{9}{8} \ln 2 \ln 3 - \frac{39}{16} \ln 3 - \frac{9}{32} \ln^2 3 \right. \\ &\quad \left. + \frac{15}{8} \text{Li}_2(1/4) \right) + C_A C_F \left( -\frac{397}{192} - \frac{7}{64} \zeta_2 - \frac{47}{8} \ln 2 + \frac{11}{8} \ln^2 2 - \frac{9}{8} \ln 2 \ln 3 \right. \\ &\quad \left. + \frac{75}{16} \ln 3 + \frac{9}{32} \ln^2 3 + \frac{3}{4} \text{Li}_2(1/4) \right) + C_F T_R \left( -\frac{55}{96} - \frac{1}{32} \zeta_2 + \frac{11}{3} \ln 2 \right. \\ &\quad \left. - \frac{3}{2} \ln 3 + \frac{7}{8} \text{Li}_2(1/4) \right) + C_F T_R n_f \left( \frac{5}{12} + \frac{1}{8} \zeta_2 \right) + c_{\varphi,20}^{(2)}, \\ c_{1,02} &= (n_c + 1) \left( -\frac{15}{128} - \frac{3}{128} \zeta_2 + c_{\varphi,02}^{(2)} \right), \\ c_{1,11} &= C_F (n_c + 1) \left( \frac{3}{8} + \frac{3}{8} \ln 2 - \frac{9}{16} \ln 3 - \frac{3}{8} \text{Li}_2(1/4) \right), \end{aligned} \quad (4.5)$$

where  $c_{\varphi,02}^{(2)}$  and  $c_{\varphi,20}^{(2)}$  are given in Eq. (3.28), and we have set  $\mu = \mu_t$  for the sake of brevity, see Eq. (3.8). The result for general values of  $\mu$  can be reconstructed from the relation

$$\mu^2 \frac{d}{d\mu^2} c_1(t) = \left[ \frac{\partial}{\partial L_{\mu t}} + \beta^s(a_s, a_\lambda) \frac{\partial}{\partial a_s} + \beta^\lambda(a_s, a_\lambda) \frac{\partial}{\partial a_\lambda} \right] c_1(t) = \gamma_{\phi^\dagger\phi} c_1(t), \quad (4.6)$$

which follows from the renormalization scale independence of the l.h.s. of Eq. (4.1). For convenience of the reader, we include the explicitly  $\mu$ -dependent terms in the ancillary file accompanying this paper, see Appendix B.

## 4.2 The Noether current

The second example we consider is the Noether current for the squark, given by the operator  $\phi^\dagger \overleftrightarrow{D}_\mu \phi$ . Its Feynman rules are

$$\begin{array}{c} \phi^\dagger D_\mu \phi \\ \otimes \\ \swarrow \quad \searrow \\ i, p \quad j, q \end{array} = i \delta_{ij} (p - q)_\mu,$$

(4.7)

$$\begin{array}{c} \phi^\dagger D_\mu \phi \\ \otimes \\ \swarrow \quad \searrow \\ i, p \quad j, q \\ \quad \quad \quad \rho, a \end{array} = 2 t_{ji}^a \delta_{\mu\rho},$$

where the momenta are assumed outgoing.

Neglecting again higher orders in  $t$ , the SFTX of the flowed version of this operator reads

$$\mathring{Z}_\varphi \varphi^\dagger(t) \overleftrightarrow{D}_\mu \varphi(t) = d(t) \phi^\dagger \overleftrightarrow{D}_\mu \phi, \tag{4.8}$$

with the coefficients up to NNLO given by

$$\begin{aligned}
 d(t) &= \sum_{n,m=0}^{\infty} d_{nm} a_s^n a_\lambda^m, \\
 d_{00} &= 1, \quad d_{10} = -C_F (1 + 2 \ln 2), \quad d_{01} = 0, \\
 d_{20} &= C_F^2 \left( \frac{111}{128} - \frac{1}{8} \zeta_2 + \frac{13}{2} \ln 2 - \frac{7}{8} \ln^2 2 + \frac{9}{8} \ln 2 \ln 3 - \frac{33}{8} \ln 3 - \frac{9}{32} \ln^2 3 \right. \\
 &\quad \left. + \frac{3}{2} \text{Li}_2(1/4) \right) + C_A C_F \left( -\frac{231}{256} - \frac{1}{8} \zeta_2 - \frac{19}{8} \ln 2 + \frac{11}{8} \ln^2 2 - \frac{9}{8} \ln 2 \ln 3 \right. \\
 &\quad \left. + \frac{21}{16} \ln 3 + \frac{9}{32} \ln^2 3 + \frac{9}{32} \text{Li}_2(1/4) \right) + C_F T_R \left( \frac{7}{128} + \frac{5}{32} n_f \right) + c_{\varphi,20}^{(2)} \\
 &\quad + d_{10} \beta_{20}^s L_{\mu t}, \\
 d_{02} &= (n_c + 1) \left( -\frac{7}{512} + c_{\varphi,02}^{(2)} \right), \\
 d_{11} &= C_F \left( -\frac{3}{16} - \frac{1}{32} \zeta_2 + \frac{9}{32} \text{Li}_2(1/4) \right),
 \end{aligned} \tag{4.9}$$

where  $c_{\varphi,20}^{(2)}$ ,  $c_{\varphi,02}^{(2)}$ , and  $\beta_{20}^s$  are given in Eqs. (3.28) and (A.3), respectively. The logarithmic term is consistent with

$$\mu^2 \frac{d}{d\mu^2} d(t) = 0, \tag{4.10}$$

which follows from the renormalization scale invariance of both the l.h.s. of Eq. (4.8) and the regular Noether current. It is worth noting that the NLO coefficient  $d_{10}$  arises completely from the ringed-scheme conversion of Eq. (3.27), while it vanishes in the  $\overline{\text{MS}}$ -scheme.

## 5 Flowed anomalous dimension

The gradient flow can be viewed as a renormalization scheme. The corresponding renormalization group equation for a set of flowed operators  $\tilde{\mathcal{O}} = (\tilde{\mathcal{O}}_1, \dots)$  in this scheme can be written as

$$t \frac{d}{dt} \tilde{\mathcal{O}}(t) = \tilde{\gamma} \tilde{\mathcal{O}}(t), \quad (5.1)$$

where the flowed anomalous dimension matrix  $\tilde{\gamma}$  can be expressed in terms of the matching matrix  $\zeta(t)$  of the SFTX, defined as

$$\tilde{\mathcal{O}}(t) = \zeta(t) \mathcal{O}. \quad (5.2)$$

Setting  $\mu^2 \sim 1/t$ , one finds [19, 22]

$$\tilde{\gamma} = \left[ \left( t \frac{\partial}{\partial t} - \beta^s \frac{\partial}{\partial a_s} - \beta^\lambda \frac{\partial}{\partial a_\lambda} \right) \zeta(t) \right] \zeta^{-1}(t) + \zeta(t) \gamma \zeta^{-1}(t), \quad (5.3)$$

where the partial derivative w.r.t.  $t$  takes into account any power-dependence of  $\zeta(t)$  on  $t$ , and  $\gamma$  is the anomalous dimension of the regular operator  $\mathcal{O}$ , i.e.<sup>4</sup>

$$\mu^2 \frac{d}{d\mu^2} \mathcal{O} = -\gamma \mathcal{O}. \quad (5.4)$$

For the Noether current in Eq. (4.8), we have

$$\begin{aligned} \tilde{\mathcal{O}}(t) &= \hat{Z}_\varphi \varphi^\dagger(t) \overleftrightarrow{D} \varphi(t), & \zeta(t) &= d(t), & \gamma &= 0, \\ \mathcal{O}(t) &= \phi^\dagger \overleftrightarrow{D} \phi(t), & t \frac{d}{dt} \tilde{\mathcal{O}}(t) &= \tilde{\gamma}_d \tilde{\mathcal{O}}(t). \end{aligned} \quad (5.5)$$

In this case, the first term in brackets of Eq. (5.3) does not contribute. Given the result in Eq. (4.9), we can determine  $\tilde{\gamma}_d$  through  $\mathcal{O}(a_s^i a_\lambda^j)$  with  $i + j = 3$ :

$$\begin{aligned} \tilde{\gamma}_d &= \sum_{n,m=0}^{\infty} \tilde{\gamma}_{d,nm} a_s^n a_\lambda^m, \\ \tilde{\gamma}_{d,00} &= \tilde{\gamma}_{d,10} = \tilde{\gamma}_{d,01} = \tilde{\gamma}_{d,11} = 0, \\ \tilde{\gamma}_{d,20} &= \beta_{20}^s d_{10}, \\ \tilde{\gamma}_{d,30} &= \beta_{30}^s d_{10} + \beta_{20}^\lambda d_{11} - \beta_{20}^s (d_{10}^2 - 2 d_{20}), \\ \tilde{\gamma}_{d,21} &= 2 \beta_{20}^\lambda d_{02} + (\beta_{11}^\lambda + \beta_{20}^s) d_{11}, \\ \tilde{\gamma}_{d,12} &= 2 \beta_{11}^\lambda d_{02} + \beta_{02}^\lambda d_{11}, \\ \tilde{\gamma}_{d,03} &= 2 \beta_{02}^\lambda d_{02}. \end{aligned} \quad (5.6)$$

---

<sup>4</sup>Note that Ref. [22] defines  $\gamma$  with the opposite sign.



In the above relations, the renormalization scale is chosen to be  $\mu = \mu_t$ , such that  $L_{\mu t} = 0$ , see Eq. (3.8); the full relation can be found in the ancillary file to this paper, see Appendix B.

For the scalar bilinear of Eq. (4.1), on the other hand, we need to take into account the mixing with the unit operator. Therefore, in this case we set

$$\begin{aligned}\tilde{\mathcal{O}}(t) &= \begin{pmatrix} \mathbb{1} \\ \mathring{Z}_\varphi \varphi^\dagger(t) \varphi(t) \end{pmatrix}, & \zeta(t) &= \begin{pmatrix} 1 & 0 \\ \frac{1}{t} c_0 & c_1(t) \end{pmatrix}, & \gamma &= \gamma_{\phi^\dagger \phi}, \\ \mathcal{O}(t) &= \begin{pmatrix} \mathbb{1} \\ Z_{\phi^\dagger \phi} \phi^\dagger \phi \end{pmatrix}, & t \frac{d}{dt} \tilde{\mathcal{O}}(t) &= \tilde{\gamma}_c \tilde{\mathcal{O}}(t).\end{aligned}\tag{5.7}$$

This leads to

$$\tilde{\gamma}_c = \begin{pmatrix} 0 & 0 \\ -\frac{1}{t} c_0 (1 + \tilde{\gamma}_1) & \tilde{\gamma}_1 \end{pmatrix} - \zeta(t) \gamma_{\phi^\dagger \phi} \zeta^{-1}(t),\tag{5.8}$$

with

$$\tilde{\gamma}_1 = - \left[ \left( \beta^s \frac{\partial}{\partial a_s} + \beta^\lambda \frac{\partial}{\partial a_\lambda} \right) c_1(t) \right] c_1^{-1}(t).\tag{5.9}$$

This can be easily expressed in terms of the coefficients  $c_{1,ij}$ ,  $\beta_{ij}^s$ , and  $\beta_{ij}^\lambda$  from Eqs. (4.5), (A.3), and (A.4), similar to Eq. (5.6).

## 6 Conclusions and Outlook

We have presented the generalization of the GFF formalism to a gauge theory with scalar particles. Aside from possible phenomenological applications, for example the Higgs sector of the SM, our results validate the consistency of the formalism in this context. We show that, similar to the fermionic case, the flowed scalar field requires renormalization, albeit only beyond NLO. In addition to the  $\overline{\text{MS}}$  scheme, we define a quasi-physical scheme for the scalar quarks, defined at non-zero flow-time, and analogous to the ringed scheme for fermions. It leads to renormalization group invariant Green's functions of the scalar field and can be implemented both perturbatively and on the lattice. We evaluate the corresponding renormalization constant through two loops.

Our results constitute an important step towards a gradient-flow description of the full SM, which paves the way for novel perspectives on calculations within Standard Model Effective Field Theory (SMEFT), for example.

**Acknowledgments.** We thank Andrei Kataev for helpful communication concerning the disagreement of Eq. (4.3) with Ref. [61]. Furthermore, we would like to thank Jonas Rongen and Aiman el Assad for preliminary work on this project. This research was supported by the *Deutsche Forschungsgemeinschaft (DFG, German Research Foundation)* under grant 460791904.

## A Renormalization constants

The couplings are renormalized by

$$\begin{aligned} a_s^B &= \left( \frac{\mu^2 e^{\gamma_E}}{4\pi} \right)^\epsilon Z_s(a_s, a_\lambda) a_s, \\ a_\lambda^B &= \left( \frac{\mu^2 e^{\gamma_E}}{4\pi} \right)^\epsilon \left[ Z_{s\lambda}(a_s) a_s + Z_\lambda(a_s, a_\lambda) a_\lambda \right], \end{aligned} \quad (\text{A.1})$$

where the dependence of the renormalized couplings  $a_s$  and  $a_\lambda$  on the renormalization scale  $\mu$  has been suppressed. It is governed by the renormalization group equations

$$\begin{aligned} \mu^2 \frac{d}{d\mu^2} a_s &= \beta^s(a_s, a_\lambda) \equiv -\epsilon a_s - \sum_{n=2}^{\infty} \sum_{i=0}^n \beta_{i,n-i}^s a_s^i a_\lambda^{n-i}, \\ \mu^2 \frac{d}{d\mu^2} a_\lambda &= \beta^\lambda(a_s, a_\lambda) \equiv -\epsilon a_\lambda - \sum_{n=2}^{\infty} \sum_{i=0}^n \beta_{i,n-i}^\lambda a_s^i a_\lambda^{n-i}. \end{aligned} \quad (\text{A.2})$$

The coefficients for the strong beta function through two-loop level, i.e.  $n = 3$ , are [64]

$$\begin{aligned} \beta_{20}^s &= \frac{1}{4} \left( \frac{11}{3} C_A - \frac{4}{3} n_f T_R - \frac{1}{3} T_R \right), \\ \beta_{30}^s &= \frac{1}{16} \left[ \frac{34}{3} C_A^2 - \left( 4C_F + \frac{20}{3} C_A \right) T_R n_f - \left( 4C_F + \frac{2}{3} C_A \right) T_R \right], \\ \beta_{ij}^s &= 0 \quad \text{otherwise,} \end{aligned} \quad (\text{A.3})$$

where  $n_f$  is the number of quark flavors, and we only take into account a single scalar quark field, see Eq. (2.1). For the scalar coupling, the coefficients through two-loop level are [61, 65]

$$\begin{aligned} \beta_{20}^\lambda &= -\frac{12C_F^2 - 3C_A C_F + 12C_F T_R}{4(n_c + 1)}, \\ \beta_{11}^\lambda &= \frac{3}{2} C_F, \quad \beta_{02}^\lambda = -\frac{1}{8} (n_c + 1) - \frac{3}{8}, \\ \beta_{ij}^\lambda &= 0 \quad \text{otherwise.} \end{aligned} \quad (\text{A.4})$$

The renormalization constants in Eq. (A.1) are then given by

$$\begin{aligned} Z_s &= 1 - a_s \frac{\beta_{20}^s}{\epsilon} - a_s^2 \left( \frac{(\beta_{20}^s)^2}{\epsilon^2} + \frac{\beta_{30}^s}{2\epsilon} \right), \\ Z_\lambda &= 1 - a_s \frac{\beta_{11}^\lambda}{\epsilon} - a_\lambda \frac{\beta_{02}^\lambda}{\epsilon}, \quad Z_{s\lambda} = -a_s \frac{\beta_{20}^\lambda}{\epsilon}. \end{aligned} \quad (\text{A.5})$$

Though well known, let us emphasize the non-multiplicativity of the  $a_\lambda$  renormalization, manifest through the non-vanishing expression for  $Z_{s\lambda}$ , and caused by diagrams like the one shown in Fig. 5.

The anomalous dimension  $\gamma$  of a particular quantity is related to the corresponding renormalization constant  $Z$  by

$$\mu^2 \frac{d}{d\mu^2} Z = -\gamma Z. \quad (\text{A.6})$$

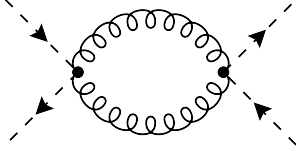


Figure 5: Example diagram for the origin of the non-multiplicative renormalization  $Z_{s\lambda}$  of the scalar coupling  $a_\lambda$ .

We write it as

$$\gamma = - \sum_{n,m=0}^{\infty} \gamma_{nm} a_s^n a_\lambda^m. \quad (\text{A.7})$$

The generic form of an (gauge independent)  $\overline{\text{MS}}$ -renormalization constant is then given by

$$\begin{aligned} Z = & 1 - a_s \frac{\gamma_{10}}{\epsilon} - a_\lambda \frac{\gamma_{01}}{\epsilon} + a_s^2 \left( \frac{1}{2\epsilon^2} \left[ \gamma_{10}^2 + \beta_{20}^\lambda \gamma_{01} + \beta_{20}^s \gamma_{10} \right] - \frac{\gamma_{20}}{2\epsilon} \right) \\ & + a_\lambda^2 \left( \frac{1}{2\epsilon^2} \left[ \gamma_{01}^2 + \beta_{02}^\lambda \gamma_{01} \right] - \frac{\gamma_{02}}{2\epsilon} \right) \\ & + a_s a_\lambda \left( \frac{1}{\epsilon^2} \left[ \gamma_{01} \gamma_{10} + \frac{\beta_{11}^\lambda \gamma_{01}}{2} \right] - \frac{\gamma_{11}}{2\epsilon} \right) + \text{h.o.} \end{aligned} \quad (\text{A.8})$$

## B Ancillary file

For the reader's convenience, we provide the results of this paper in an ancillary file in `Mathematica` format. A list of the results and their corresponding expressions in the ancillary file is found in Appendix B.

The mixing coefficients  $c_1$  and  $d$  are provided in both the ringed scheme of the scalar quarks as well as in the  $\overline{\text{MS}}$  scheme. The parameter `Xzetaphi` allows to switch between the schemes; setting `Xzetaphi=0/1` corresponds to the  $\overline{\text{MS}}$ /ringed scheme. The flowed anomalous dimension  $\tilde{\gamma}_d$  is only given in the ringed scheme.

The results depend on the variables listed in Appendix B. Results in the ringed scheme depend on the numerically known coefficients  $c_{\varphi,02}^{(2)}$  and  $c_{\varphi,20}^{(2)}$  (see Eq. (3.28)). They can be inserted by applying the `Mathematica` replacement rule `ReplaceC2`.

Table 1: The expressions of the ancillary file that encode the main results of this paper.

expression	meaning	reference
<b>Et</b>	$E(t)$	Eq. (3.6)
<b>zetachi</b>	$\zeta_\chi$	Eq. (3.20)
<b>gammaphi</b>	$\gamma_{\phi^\dagger\phi}$	Eq. (4.3), Eq. (A.7)
<b>Zphi</b>	$Z_{\phi^\dagger\phi}$	Eq. (4.1)
<b>gammaphi</b>	$\gamma_\varphi$	Eq. (3.26), Eq. (A.7)
<b>Zphi</b>	$Z_\varphi$	Eq. (3.25)
<b>zetaphi</b>	$\zeta_\varphi$	Eq. (3.27)
<b>c1</b>	$c_1(t)$	Eq. (4.1)
<b>d</b>	$d(t)$	Eq. (4.8)
<b>tildegammad</b>	$\tilde{\gamma}_d$	Eq. (5.6)

Table 2: Notation for the variables in the ancillary file.

symbol	meaning	definition
<b>nc1</b>	$n_c + 1$	Section 3
<b>tr</b>	$T_R$	Eq. (2.4)
<b>cf</b>	$C_F$	Eq. (3.10)
<b>ca</b>	$C_A$	Eq. (3.10)
<b>na</b>	$n_A$	Section 3
<b>Lmut</b>	$L_{\mu t}$	Eq. (3.8)
<b>as</b>	$a_s$	Eq. (2.5)
<b>al</b>	$a_\lambda$	Eq. (2.5)
<b>nf</b>	$n_f$	Eq. (2.1)
<b>ep</b>	$\epsilon$	Section 3.1

## References

- [1] R. Narayanan and H. Neuberger, *Infinite  $N$  phase transitions in continuum Wilson loop operators*, *JHEP* **03** (2006) 064, arXiv:hep-th/0601210.
- [2] M. Lüscher, *Properties and uses of the Wilson flow in lattice QCD*, *JHEP* **08** (2010) 071, arXiv:1006.4518 [hep-lat]. [Erratum: *JHEP* 03, 092 (2014)].
- [3] M. Lüscher, *Trivializing maps, the Wilson flow and the HMC algorithm*, *Commun. Math. Phys.* **293** (2010) 899–919, arXiv:0907.5491 [hep-lat].
- [4] M. Lüscher and P. Weisz, *Perturbative analysis of the gradient flow in non-abelian gauge theories*, *JHEP* **02** (2011) 051, arXiv:1101.0963 [hep-th].
- [5] M. Lüscher, *Chiral symmetry and the Yang–Mills gradient flow*, *JHEP* **04** (2013) 123, arXiv:1302.5246 [hep-lat].
- [6] BMW collaboration, S. Borsányi, S. Dürr, Z. Fodor, C. Hoelbling, S. D. Katz, S. Krieg, T. Kurth, L. Lellouch, T. Lippert, and C. McNeile, *High-precision scale setting in lattice QCD*, *JHEP* **09** (2012) 010, arXiv:1203.4469 [hep-lat].
- [7] H. Makino and H. Suzuki, *Lattice energy–momentum tensor from the Yang–Mills gradient flow—inclusion of fermion fields*, *PTEP* **2014** (2014) 063B02, arXiv:1403.4772 [hep-lat]. [Erratum: *PTEP* 2015, 079202 (2015)].
- [8] H. Suzuki, *Energy–momentum tensor from the Yang–Mills gradient flow*, *PTEP* **2013** (2013) 083B03, arXiv:1304.0533 [hep-lat]. [Erratum: *PTEP* 2015, 079201 (2015)].
- [9] A. Shindler, *Moments of parton distribution functions of any order from lattice QCD*, *Phys. Rev. D* **110** no. 5, (2024) L051503, arXiv:2311.18704 [hep-lat].
- [10] A. Francis, P. Fritzscht, R. Karur, J. Kim, G. Pederiva, D. A. Pefkou, A. Rago, A. Shindler, A. Walker-Loud, and S. Zafeiropoulos, *Probing higher moments of pion parton distribution functions*, in *41st International Symposium on Lattice Field Theory*. 12, 2024. arXiv:2412.01750 [hep-lat].
- [11] WHOT-QCD collaboration, Y. Taniguchi, S. Ejiri, K. Kanaya, M. Kitazawa, H. Suzuki, and T. Umeda,  *$N_f = 2+1$  QCD thermodynamics with gradient flow using two-loop matching coefficients*, *Phys. Rev. D* **102** no. 1, (2020) 014510, arXiv:2005.00251 [hep-lat]. [Erratum: *Phys.Rev.D* 102, 059903 (2020)].
- [12] A. Suzuki, Y. Taniguchi, H. Suzuki, and K. Kanaya, *Four quark operators for kaon bag parameter with gradient flow*, *Phys. Rev. D* **102** no. 3, (2020) 034508, arXiv:2006.06999 [hep-lat].
- [13] M. Black, R. Harlander, F. Lange, A. Rago, A. Shindler, and O. Witzel, *Using gradient flow to renormalise matrix elements for meson mixing and lifetimes*, *PoS LATTICE2023* (2024) 263, arXiv:2310.18059 [hep-lat].

- [14] M. Black, R. Harlander, F. Lange, A. Rago, A. Shindler, and O. Witzel, *Gradient flow renormalisation for meson mixing and lifetimes*, in *41st International Symposium on Lattice Field Theory*. 9, 2024. [arXiv:2409.18891 \[hep-lat\]](#).
- [15] SymLat collaboration, J. Kim, T. Luu, M. D. Rizik, and A. Shindler, *Nonperturbative renormalization of the quark chromoelectric dipole moment with the gradient flow: Power divergences*, *Phys. Rev. D* **104** no. 7, (2021) 074516, [arXiv:2106.07633 \[hep-lat\]](#).
- [16] R. V. Harlander and T. Neumann, *The perturbative QCD gradient flow to three loops*, *JHEP* **06** (2016) 161, [arXiv:1606.03756 \[hep-ph\]](#).
- [17] R. V. Harlander, Y. Kluth, and F. Lange, *The two-loop energy-momentum tensor within the gradient-flow formalism*, *Eur. Phys. J. C* **78** no. 11, (2018) 944, [arXiv:1808.09837 \[hep-lat\]](#). [Erratum: *Eur.Phys.J.C* 79, 858 (2019)].
- [18] J. Artz, R. V. Harlander, F. Lange, T. Neumann, and M. Prausa, *Results and techniques for higher order calculations within the gradient-flow formalism*, *JHEP* **06** (2019) 121, [arXiv:1905.00882 \[hep-lat\]](#). [Erratum: *JHEP* 10, 032 (2019)].
- [19] R. V. Harlander, F. Lange, and T. Neumann, *Hadronic vacuum polarization using gradient flow*, *JHEP* **08** (2020) 109, [arXiv:2007.01057 \[hep-lat\]](#).
- [20] R. V. Harlander and F. Lange, *Effective electroweak Hamiltonian in the gradient-flow formalism*, *Phys. Rev. D* **105** no. 7, (2022) L071504, [arXiv:2201.08618 \[hep-lat\]](#).
- [21] R. Harlander, M. D. Rizik, J. Borgulat, and A. Shindler, *Two-loop matching of the chromo-magnetic dipole operator with the gradient flow*, *PoS LATTICE2022* (2023) 313, [arXiv:2212.09824 \[hep-lat\]](#).
- [22] J. Borgulat, R. V. Harlander, J. T. Kohnen, and F. Lange, *Short-flow-time expansion of quark bilinears through next-to-next-to-leading order QCD*, *JHEP* **05** (2024) 179, [arXiv:2311.16799 \[hep-lat\]](#).
- [23] R. V. Harlander, T. Nellopoulos, A. Olsson, and M. Wesle, *ftint: Calculating gradient-flow integrals with pySecDec*, [arXiv:2407.16529 \[hep-ph\]](#).
- [24] K. Kikuchi and T. Onogi, *Generalized gradient flow equation and its application to super Yang-Mills theory*, *JHEP* **11** (2014) 094, [arXiv:1408.2185 \[hep-th\]](#).
- [25] K. Hieda, A. Kasai, H. Makino, and H. Suzuki, *4D  $\mathcal{N} = 1$  SYM supercurrent in terms of the gradient flow*, *PTEP* **2017** no. 6, (2017) 063B03, [arXiv:1703.04802 \[hep-lat\]](#).
- [26] S. Aoki, K. Kikuchi, and T. Onogi, *Flow equation of  $\mathcal{N} = 1$  supersymmetric  $O(N)$  nonlinear sigma model in two dimensions*, *JHEP* **02** (2018) 128, [arXiv:1704.03717 \[hep-th\]](#).

- [27] A. Kasai, O. Morikawa, and H. Suzuki, *Gradient flow representation of the four-dimensional  $\mathcal{N} = 2$  super Yang–Mills supercurrent*, *PTEP* **2018** no. 11, (2018) 113B02, [arXiv:1808.07300 \[hep-lat\]](#).
- [28] D. Kadoh and N. Ukita, *Supersymmetric gradient flow in  $\mathcal{N} = 1$  SYM*, *Eur. Phys. J. C* **82** no. 5, (2022) 435, [arXiv:1812.02351 \[hep-th\]](#).
- [29] G. Bergner, C. López, and S. Piemonte, *Study of center and chiral symmetry realization in thermal  $\mathcal{N} = 1$  super Yang–Mills theory using the gradient flow*, *Phys. Rev. D* **100** no. 7, (2019) 074501, [arXiv:1902.08469 \[hep-lat\]](#).
- [30] D. Kadoh, K. Kikuchi, and N. Ukita, *Supersymmetric gradient flow in the Wess–Zumino model*, *Phys. Rev. D* **100** no. 1, (2019) 014501, [arXiv:1904.06582 \[hep-th\]](#).
- [31] D. Kadoh and N. Ukita, *Supersymmetric gradient flow in 4d  $\mathcal{N} = 1$  SQCD*, *Eur. Phys. J. ST* **232** no. 3, (2023) 359–364, [arXiv:2208.02467 \[hep-th\]](#).
- [32] C. Monahan and K. Orginos, *Locally smeared operator product expansions in scalar field theory*, *Phys. Rev. D* **91** no. 7, (2015) 074513, [arXiv:1501.05348 \[hep-lat\]](#).
- [33] S. Aoki, J. Balog, T. Onogi, and P. Weisz, *Flow equation for the large  $N$  scalar model and induced geometries*, *PTEP* **2016** no. 8, (2016) 083B04, [arXiv:1605.02413 \[hep-th\]](#).
- [34] S. Aoki, J. Balog, T. Onogi, and P. Weisz, *Flow equation for the scalar model in the large  $N$  expansion and its applications*, *PTEP* **2017** no. 4, (2017) 043B01, [arXiv:1701.00046 \[hep-th\]](#).
- [35] LatCos collaboration, L. Del Debbio, E. Dobson, A. Jüttner, B. Kitching-Morley, J. K. L. Lee, V. Nourry, A. Portelli, H. B. Rocha, and K. Skenderis, *Renormalisation of the energy-momentum tensor in three-dimensional scalar  $SU(N)$  theories using the Wilson flow*, *Phys. Rev. D* **103** no. 11, (2021) 114501, [arXiv:2009.14767 \[hep-lat\]](#).
- [36] Y. Abe, Y. Hamada, and J. Haruna, *Fixed point structure of the gradient flow exact renormalization group for scalar field theories*, *PTEP* **2022** no. 3, (2022) 033B03, [arXiv:2201.04111 \[hep-th\]](#).
- [37] R. V. Harlander, S. Y. Klein, and M. Lipp, *FeynGame*, *Comput. Phys. Commun.* **256** (2020) 107465, [arXiv:2003.00896 \[physics.ed-ph\]](#).
- [38] R. Harlander, S. Y. Klein, and M. C. Schaaf, *FeynGame-2.1 – Feynman diagrams made easy*, *PoS EPS-HEP2023* (2024) 657, [arXiv:2401.12778 \[hep-ph\]](#).
- [39] L. Bündgen, R. V. Harlander, S. Y. Klein, and M. C. Schaaf, *FeynGame 3.0*, [arXiv:2501.04651 \[hep-ph\]](#).
- [40] T. Steudtner and A. E. Thomsen, *General quartic  $\beta$ -function at three loops*, *JHEP* **10** (2024) 163, [arXiv:2408.05267 \[hep-ph\]](#).

- [41] A. Hasenfratz, C. T. Peterson, J. van Sickle, and O. Witzel,  $\Lambda$  parameter of the  $SU(3)$  Yang-Mills theory from the continuous  $\beta$  function, *Phys. Rev. D* **108** no. 1, (2023) 014502, [arXiv:2303.00704 \[hep-lat\]](#).
- [42] C. H. Wong, S. Borsanyi, Z. Fodor, K. Holland, and J. Kuti, *Toward a novel determination of the strong QCD coupling at the Z-pole*, *PoS LATTICE2022* (2023) 043, [arXiv:2301.06611 \[hep-lat\]](#).
- [43] P. Nogueira, *Automatic Feynman graph generation*, *J. Comput. Phys.* **105** (1993) 279–289.
- [44] P. Nogueira, *Abusing QGRAF*, *Nucl. Instrum. Meth. A* **559** (2006) 220–223.
- [45] M. Gerlach, F. Herren, and M. Lang, *tapir: A tool for topologies, amplitudes, partial fraction decomposition and input for reductions*, *Comput. Phys. Commun.* **282** (2023) 108544, [arXiv:2201.05618 \[hep-ph\]](#).
- [46] R. Harlander, T. Seidensticker, and M. Steinhauser, *Corrections of  $\mathcal{O}(\alpha_s)$  to the decay of the Z boson into bottom quarks*, *Phys. Lett. B* **426** (1998) 125–132, [arXiv:hep-ph/9712228](#).
- [47] J. A. M. Vermaseren, *New features of FORM*, [arXiv:math-ph/0010025](#).
- [48] J. Kuipers, T. Ueda, J. A. M. Vermaseren, and J. Vollinga, *FORM version 4.0*, *Comput. Phys. Commun.* **184** (2013) 1453–1467, [arXiv:1203.6543 \[cs.SC\]](#).
- [49] P. Maierhöfer, J. Usovitsch, and P. Uwer, *Kira—A Feynman integral reduction program*, *Comput. Phys. Commun.* **230** (2018) 99–112, [arXiv:1705.05610 \[hep-ph\]](#).
- [50] P. Maierhöfer and J. Usovitsch, *Kira 1.2 Release Notes*, [arXiv:1812.01491 \[hep-ph\]](#).
- [51] J. Klappert and F. Lange, *Reconstructing rational functions with FireFly*, *Comput. Phys. Commun.* **247** (2020) 106951, [arXiv:1904.00009 \[cs.SC\]](#).
- [52] J. Klappert, F. Lange, P. Maierhöfer, and J. Usovitsch, *Integral reduction with Kira 2.0 and finite field methods*, *Comput. Phys. Commun.* **266** (2021) 108024, [arXiv:2008.06494 \[hep-ph\]](#).
- [53] J. Klappert, S. Y. Klein, and F. Lange, *Interpolation of dense and sparse rational functions and other improvements in FireFly*, *Comput. Phys. Commun.* **264** (2021) 107968, [arXiv:2004.01463 \[cs.MS\]](#).
- [54] S. Borowka, G. Heinrich, S. P. Jones, M. Kerner, J. Schlenk, and T. Zirke, *SecDec-3.0: numerical evaluation of multi-scale integrals beyond one loop*, *Comput. Phys. Commun.* **196** (2015) 470–491, [arXiv:1502.06595 \[hep-ph\]](#).
- [55] S. Borowka, G. Heinrich, S. Jahn, S. P. Jones, M. Kerner, J. Schlenk, and T. Zirke, *pySecDec: a toolbox for the numerical evaluation of multi-scale integrals*, *Comput. Phys. Commun.* **222** (2018) 313–326, [arXiv:1703.09692 \[hep-ph\]](#).



- [56] S. Borowka, G. Heinrich, S. Jahn, S. P. Jones, M. Kerner, and J. Schlenk, *A GPU compatible quasi-Monte Carlo integrator interfaced to pySecDec*, *Comput. Phys. Commun.* **240** (2019) 120–137, [arXiv:1811.11720](#) [[physics.comp-ph](#)].
- [57] G. Heinrich, S. P. Jones, M. Kerner, V. Magerya, A. Olsson, and J. Schlenk, *Numerical scattering amplitudes with pySecDec*, *Comput. Phys. Commun.* **295** (2024) 108956, [arXiv:2305.19768](#) [[hep-ph](#)].
- [58] T. Binoth and G. Heinrich, *An automatized algorithm to compute infrared divergent multiloop integrals*, *Nucl. Phys. B* **585** (2000) 741–759, [arXiv:hep-ph/0004013](#).
- [59] T. Binoth and G. Heinrich, *Numerical evaluation of multiloop integrals by sector decomposition*, *Nucl. Phys. B* **680** (2004) 375–388, [arXiv:hep-ph/0305234](#).
- [60] S. G. Gorishnii, S. A. Larin, and F. V. Tkachov, *The algorithm for OPE coefficient functions in the MS scheme*, *Phys. Lett. B* **124** (1983) 217–220.
- [61] S. G. Gorishnii, A. L. Kataev, and S. A. Larin, *Two loop renormalization group calculations in theories with scalar quarks*, *Theor. Math. Phys.* **70** (1987) 262–270.
- [62] M. E. Machacek and M. T. Vaughn, *Two loop renormalization group equations in a general quantum field theory. 3. Scalar quartic couplings*, *Nucl. Phys. B* **249** (1985) 70–92.
- [63] M. Luo and Y. Xiao, *Two loop renormalization group equations in the standard model*, *Phys. Rev. Lett.* **90** (2003) 011601, [arXiv:hep-ph/0207271](#).
- [64] D. R. T. Jones, *Asymptotic behaviour of supersymmetric Yang-Mills theories in the two-loop approximation*, *Nuclear Physics B* **87** no. 1, (1975) 127–132.
- [65] D. J. Gross and F. Wilczek, *Asymptotically free gauge theories. I*, *Phys. Rev. D* **8** (Nov, 1973) 3633–3652.